Proceedings of the 1998 IEEE
International Conference on Robotics & Automation
Leuven, Belgium • May 1998

Dynamic Model of A Gyroscopic Wheel

Gora C. Nandy[1,2] and Yangsheng Xu[1,3]

[1]Department of Mechanical and Automation Engineering, The Chinese University of Hong Kong, Hong Kong
[2]Mechanical Engineering Deparment, REC, Durgapur-713 209, India
[3]The Robotics Institute, Carnegie Mellon University, Pittsburgh, PA 15213, USA

Abstract

In this paper, we develop a dynamic model of a gyroscopic wheel, an important component of Gyrover, a single-wheel robot developed at Carnegie Mellon University. The Gyrover robot consists of a single wheel, and is actuated through a spinning flywheel attached through a two-link manipulator at the wheel bearing. The flywheel can be tilted to achieve steering, and can be driven forwards and backwards to accelerate the robot. As a first step in modeling this highly coupled, dynamically stable system, this paper focuses on developing a 3D model of the wheel part of the Gyrover. In this paper, we first describe the Gyrover robot. We then develop the dynamic model of the wheel through the Lagrangian constrained generalized formulation. Finally, we implement the resulting equations of motion and present simulation results for the unactuated Gyrover in the different gravitational environments of earth, the moon, and Mars.

1. Introduction

Gyrover is a novel, single wheel gyroscopically stabilized robot, originally developed at Carnegie Mellon University [1]. Two prototypes have already been developed, with a third currently under construction; Figures 1 and 2 show a schematic and photograph of the first prototype. Essentially, Gyrover is a sharp-edged wheel, with an actuation mechanism fitted inside the wheel. The actuation mechanism consists of three separate actuators: (1) a *spin motor*, which spins a suspended flywheel at a high rate, imparting dynamic stability to the robot; (2) a *tilt motor*, which controls the angle of the spinning flywheel, and ultimately controls the steering of Gyrover; and (3) a *drive motor*, which causes forward and/or backward acceleration, by shifting Gyrover's internal pendulum mass.

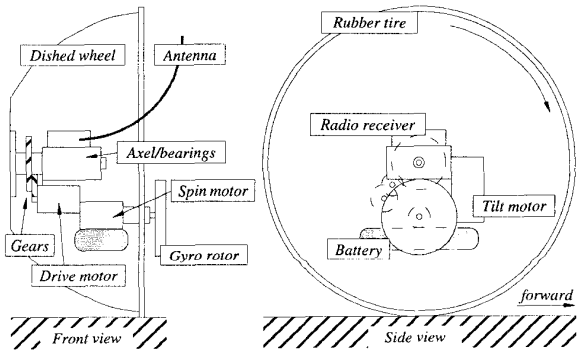

Fig. 1: A diagram of the first prototype of the Gyrover.

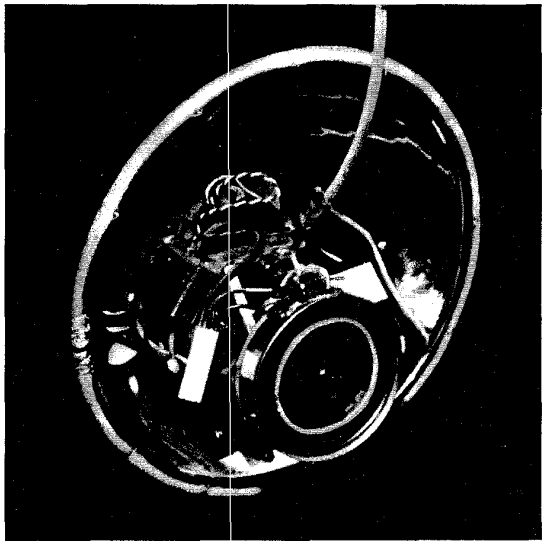

Fig. 2: Photograph of the first prototype of the Gyrover.

The behavior of Gyrover is based on the principle of gyroscopic precession as exhibited in the stability of a rolling wheel. Because of its angular momentum, a spinning wheel tends to precess at right angles to an applied torque. Therefore, when a rolling wheel leans to one side, rather than just fall over, the gravitationally induced torque causes the wheel to precess so that it turns in the direction that it is leaning.

As a concept, Gyrover has a number of potential advantages over multi-wheeled vehicles:

1. The entire system can be enclosed within the wheel to provide mechanical and environmental protection for the equipment and actuation mechanism.
2. Gyrover is resistant to getting stuck on obstacles because it has no body to hang up, no exposed appendages (in principle), and the entire exposed surface is driven.
3. In manual control experiments, we have shown that

the tiltable flywheel can be used to right the vehicle from its statically stable rest position (on its side).

4. Gyrover can turn in place by simply leaning and precessing in the desired direction, with no special steering mechanism, thus enhancing maneuverability.
5. Single-point contact with the ground eliminates the need to accommodate uneven surfaces and potentially simplifies control.
6. Full drive traction is available because all the weight is on the single drive wheel.

Potential applications for Gyrover are numerous. We have shown that Gyrover can travel on both land and water; thus, it may find amphibious use on beaches or swampy areas, for general transportation, exploration, rescue or recreation. Similarly, with appropriate tread, it should travel well over soft snow with good traction and minimal rolling resistance. As a surveillance robot, Gyrover could use its slim profile to pass through doorways and narrow passages, and also use its ability to turn in place to maneuver in tight quarters. Another potential application is as a high-speed lunar vehicle, where the absence of aerodynamic disturbances and low gravity would permit efficient, high-speed mobility.

Thus far, the Gyrover robots have been controlled only manually, using two joysticks to control the drive and spin motors through a radio link. This is the case in part because no complete dynamic model of Gyrover has as of yet been developed. Developing such a dynamic model, while apparently tractable, involves the inherent complexities of modeling two coupled, rotating masses whose axes of rotation are misaligned in 3-dimensional space.

This paper takes the important first step in developing a complete 3-dimensional dynamic model of Gyrover by first deriving the equations of motion of an unactuated Gyrover, or in other words, a single gyroscopic wheel. A companion paper [2] subsequently incorporates the actuation mechanism with the dynamic model developed herein.

Thus, in this paper, we first provide a description of the Gyrover robot. Next, assuming rolling without slip, and point contact on a flat surface, we derive the nonholonomic constraints for a single gyroscopic wheel without actuation. We then derive the equations of motions for the wheel using the constrained generalized Lagrangian principle. Finally, we implement the dynamic equations in a real-time graphic simulator and report results for different gravitational environments, including earth, the moon and Mars.

2. Constraints of motions

2.1 Nonholonomic constraints

Rolling without slipping is a typical example of a nonholonomic system, since in most cases, some of the constrained equations for the system are nonintegrable. Thus, Gyrover is a nonholonomic system. A number of techniques for analyzing nonholonomic systems have been developed [3-7]; the *Lagrangian constrained generalized principle* is one of the better know of these methods, and we use it below for deriving the dynamic model of a gyroscopic wheel.

Let us represent a system with m generalized coordinates as,

$$q_j = (q_1, q_2, \ldots, q_m),\ j \in \{1, 2, \ldots, m\} \tag{1}$$

acted on by a set of m generalized forces given by,

$$Q_j = (Q_1, Q_2, \ldots, Q_m),\ j \in \{1, 2, \ldots, m\} \tag{2}$$

In nonholonomic systems the number of generalized coordinates exceeds the number of degrees of freedom. If there are n degrees of freedom and m generalized coordinates, there will be $(m-n)$ constraint conditions that must explicitly be satisfied by the system. In functional form, the constrained equations can be written as,

$$f_s = f_s(q) = f_s(q_1, q_2, \ldots, q_m, t) = 0. \tag{3}$$

We can write the corresponding time derivatives as,

$$\dot{f}_s = \sum_{j=1}^{m} \frac{\partial}{\partial q_j} f_s(q_1, q_2, \ldots, q_m, t)\dot{q}_j + \frac{\partial}{\partial t} f_s(q) = 0, \tag{4}$$

or, in more general form,

$$\sum_{j=1}^{m} A_{sj}\dot{q}_j + a_s = 0,\ s \in \{1, 2, \ldots, m-n\}. \tag{5}$$

For a nonholonomic system, the set of Lagrangian equations are then given by,

$$\frac{d}{dt}\left(\frac{\partial L}{\partial \dot{q}_j}\right) - \frac{\partial L}{\partial q_j} = \sum_{s=1}^{m-n} \lambda_s A_{sj},\ j \in \{1, 2, \ldots, m\} \tag{6}$$

where $L = T - P$ is the Lagrangian function, T is the total kinetic energy of the system, P is the total potential energy of the system, and each λ_s is a Lagrangian multiplier which accounts for the system constraints.

To represent the Gyrover wheel, we require six coordinates, three for position (X, Y, Z) and three for orientation (α, β, γ). The Euler angles (α, β, γ) represent the precession, lean and spin angles of the wheel, respectively, and are illustrated in Figure 3.

2.2 Coordinate transformation

For the discussion below, let the inertial frame $\{X, Y, Z\}$ be attached to the ground x-y plane, which represents a perfectly flat surface upon which the Gyrover wheel rolls (see Figure 4). Let the body coordinate frame $\{x_B, y_B, z_B\}$ be attached to the mass center of the wheel, where z_B represents axis of rotation for the wheel. The composite rotation matrix which transforms the wheel from *state* 1 to *state* 2 in Figure 4 is given by R_c,

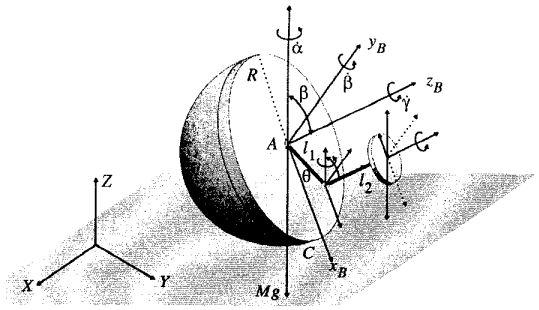

Fig. 3: Definition of system variables for Gyrover.

$$R_c = R_{(X,-\pi/2)}R_{(z_B,\pi)}R_{(x_B,-\alpha)}R_{y_B,-(\pi/2-\beta)} \tag{7}$$

$$R_c = \begin{bmatrix} -s\alpha c\beta & -c\alpha & -s\alpha s\beta \\ c\alpha c\beta & -s\alpha & c\alpha s\beta \\ -s\beta & 0 & c\beta \end{bmatrix} \tag{8}$$

where $c\alpha = \cos\alpha$, $s\alpha = \sin\alpha$, $c\beta = \cos\beta$ and $s\beta = \sin\beta$.

Now, denote $\{i, j, k\}$ and $\{l, m, n\}$ as the unit vectors along the x, y and z axes of the inertial and body frames, respectively. Then, the relationship $\{i, j, k\}$ between $\{l, m, n\}$ is given by,

$$l = -(s\alpha c\beta)i + (c\alpha c\beta)j - s\beta k \tag{9}$$

$$m = -(c\alpha)i - (s\alpha)j \tag{10}$$

$$n = -(s\alpha s\beta)i + c\alpha s\beta j + c\beta k. \tag{11}$$

2.3 Velocity constraints

Below, we derive a general expression for v_A, the velocity of the wheel's center. First, we note that,

$$\omega_B = \omega_x l + \omega_y m + \omega_z n = -\dot{\alpha}s\beta l + \dot{\beta}m + (\dot{\gamma} + \dot{\alpha}c\beta)n \tag{12}$$

where ω_B is the angular velocity of the wheel. Now, we can express v_A as,

$$v_A = \omega_B \times r_{A \leftarrow C} + v_C \tag{13}$$

where v_C is the velocity of the contact point and $r_{A \leftarrow C} = \{-Rl\}$ represents the vector from C to A in Figure 3. If we assume perfect rolling without slip, $v_C = 0$ and (13) reduces to,

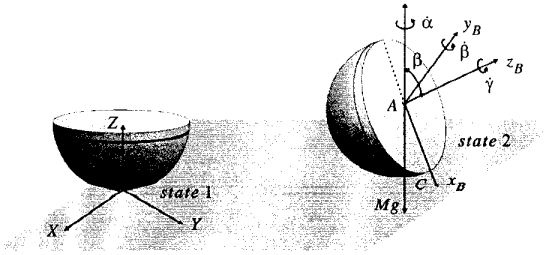

Fig. 4: Coordinate transformation from the inertial to the body coordinate frames.

$$v_A = \omega_B \times r_{A \leftarrow C} \tag{14}$$

$$v_A = \{-\dot{\alpha}s\beta l + \dot{\beta}m + (\dot{\gamma} + \dot{\alpha}c\beta)n\} \times \{-Rl\} \tag{15}$$

$$v_A = -R(\dot{\gamma} + \dot{\alpha}c\beta)m + R\dot{\beta}n \tag{16}$$

Transforming (16) to the inertial frame, we get the following expression for v_A:

$$v_A = \dot{X}i + \dot{Y}j + \dot{Z}k, \tag{17}$$

where,

$$\dot{X} = R(\dot{\gamma}c\alpha + \dot{\alpha}c\alpha c\beta - \dot{\beta}s\alpha s\beta) \tag{18}$$

$$\dot{Y} = R(\dot{\gamma}s\alpha + \dot{\alpha}c\beta s\alpha + \dot{\beta}c\alpha s\beta) \tag{19}$$

$$\dot{Z} = R\dot{\beta}c\beta \tag{20}$$

Equations (18) through (20) represent the three velocity constraint equations. The first two equations are nonintegrable and therefore nonholonomic constraint equations of the type given in (5). The last equation, however, is integrable and leads to the simple geometric or holonomic constraint,

$$Z = Rs\beta, \tag{21}$$

assuming initial conditions $Z_0 = 0$ and $\beta_0 = 0$. Therefore, we can represent Gyrover through five, rather than six independent coordinates (e.g. $\{X, Y, \alpha, \beta, \gamma\}$ or $\{X, Y, Z, \alpha, \gamma\}$).

3. Dynamic model

3.1 Equations of motion

We now derive the equations of motion by calculating the Lagrangian $L = T - P$ of the system, where T is the total kinetic energy of the system given by,

$$T = \frac{1}{2}M(\dot{X}^2 + \dot{Y}^2 + \dot{Z}^2) + \frac{1}{2}(I_{xx}\omega_x^2 + I_{yy}\omega_y^2 + I_{zz}\omega_z^2) \tag{22}$$

and P represents the potential energy of the system given by,

$$P = MgR\sin\beta. \tag{23}$$

Assuming the Gyrover wheel to be hemispherical,

$$I_{xx} = I_{yy} = (5/8)I_{zz},\ I_{zz} = (2/5)MR^2, \tag{24}$$

where M is the mass of the wheel and R is its radius. The Lagrangian function in terms of the constrained generalized coordinates then becomes,

$$L = \frac{1}{2}M\Big[\dot{X}^2 + \dot{Y}^2 + \dot{Z}^2 + \frac{1}{4}(R\dot{\alpha}s\beta)^2 + \frac{1}{4}(R\dot{\beta})^2 + \frac{2}{5}R^2(\dot{\alpha}c\beta + \dot{\gamma})^2\Big] - MgRs\beta \tag{25}$$

From equations (5) and (6), we determine the Lagrangian equations of motion by evaluating the following expressions:

$$\frac{\partial L}{\partial \dot{X}} = M\dot{X}, \frac{d}{dt}\left(\frac{\partial L}{\partial \dot{X}}\right) = M\ddot{X}, \frac{\partial L}{\partial X} = 0 \tag{26}$$

$$\frac{\partial L}{\partial \dot{Y}} = M\dot{Y}, \frac{d}{dt}\left(\frac{\partial L}{\partial \dot{Y}}\right) = M\ddot{Y}, \frac{\partial L}{\partial Y} = 0 \tag{27}$$

$$\frac{\partial L}{\partial \dot{\alpha}} = MR^2\left[\frac{1}{4}\dot{\alpha}s\beta^2 + \frac{2}{5}(\dot{\gamma} + \dot{\alpha}c\beta)c\beta\right],$$

$$\frac{d}{dt}\left(\frac{\partial L}{\partial \dot{\alpha}}\right) = MR^2\left[\ddot{\alpha}\left(\frac{2}{5}c\beta^2 + \frac{1}{4}s\beta^2\right) + \frac{2}{5}\ddot{\gamma}c\beta - \frac{2}{5}\dot{\beta}\dot{\gamma}s\beta - \frac{2}{5}\dot{\alpha}\dot{\beta}c\beta s\beta\right],$$

$$\frac{\partial L}{\partial \alpha} = 0 \tag{28}$$

$$\frac{\partial L}{\partial \dot{\beta}} = \frac{1}{4}MR^2\dot{\beta}, \frac{d}{dt}\left(\frac{\partial L}{\partial \dot{\beta}}\right) = \frac{1}{4}MR^2\ddot{\beta},$$

$$\frac{\partial L}{\partial \beta} = -MR^2\dot{\alpha}\left[\frac{3}{20}\dot{\alpha}c\beta + \frac{2}{5}\dot{\gamma}\right]s\beta - MgRc\beta \tag{29}$$

$$\frac{\partial L}{\partial \dot{\gamma}} = \frac{2}{5}MR^2(\dot{\alpha}c\beta + \dot{\gamma}),$$

$$\frac{d}{dt}\left(\frac{\partial L}{\partial \dot{\gamma}}\right) = \frac{2}{5}MR^2(\ddot{\gamma} - \dot{\alpha}\dot{\beta}s\beta + \ddot{\alpha}c\beta), \frac{\partial L}{\partial \gamma} = 0 \tag{30}$$

$$M\ddot{x} = \lambda_1 A_{11} + \lambda_2 A_{21} \tag{31}$$

$$M\ddot{y} = \lambda_1 A_{12} + \lambda_2 A_{22} \tag{32}$$

$$MR^2\left[\ddot{\alpha}\left(\frac{2}{5}c\beta^2 + \frac{1}{4}s\beta^2\right) + \frac{2}{5}\ddot{\gamma}c\beta - \frac{2}{5}\dot{\beta}\dot{\gamma}s\beta - \frac{2}{5}\dot{\alpha}\dot{\beta}c\beta s\beta\right] = \lambda_1 A_{13} + \lambda_2 A_{23} \tag{33}$$

$$\frac{1}{4}MR^2\ddot{\beta} + MR^2\dot{\alpha}\left[\frac{3}{20}\dot{\alpha}c\beta + \frac{2}{5}\dot{\gamma}\right]s\beta + MgRc\beta = \lambda_1 A_{14} + \lambda_2 A_{24} \tag{34}$$

$$\frac{2}{5}MR^2(\ddot{\gamma} - \dot{\alpha}\dot{\beta}\sin\beta + \ddot{\alpha}\cos\beta) = \lambda_1 A_{15} + \lambda_2 A_{25} \tag{35}$$

$$A_{11}\dot{X} + A_{12}\dot{Y} + A_{13}\dot{\alpha} + A_{14}\dot{\beta} + A_{15}\dot{\gamma} + a_1 = 0 \tag{36}$$

$$A_{21}\dot{X} + A_{22}\dot{Y} + A_{23}\dot{\alpha} + A_{24}\dot{\beta} + A_{25}\dot{\gamma} + a_2 = 0 \tag{37}$$

Comparing the constraint equations (18) and (19) with (36) and (37) we have that,

$$A_{11} = 1, A_{12} = 0, A_{13} = -Rc\alpha c\beta,$$
$$A_{14} = Rs\alpha s\beta, A_{15} = -Rc\alpha, a_1 = 0 \tag{38}$$
$$A_{21} = 0, A_{22} = 1, A_{23} = -Rc\alpha s\beta,$$
$$A_{24} = -Rc\alpha s\beta, A_{25} = -Rs\alpha, a_2 = 0 \tag{39}$$

Thus from (6), the Lagrangian's equations of motion are,

$$M\ddot{X} = \lambda_1 \tag{40}$$

$$M\ddot{Y} = \lambda_2 \tag{41}$$

$$MR^2\left[\ddot{\alpha}\left(\frac{2}{5}c\beta^2 - \frac{1}{4}s\beta^2\right) + \frac{2}{5}\ddot{\gamma}c\beta - \frac{2}{5}\dot{\beta}\dot{\gamma}s\beta - \frac{2}{5}\dot{\alpha}\dot{\beta}c\beta s\beta\right] = -\lambda_1 Rc\alpha c\beta - \lambda_2 Rs\alpha c\beta \tag{42}$$

$$\frac{1}{4}MR^2\ddot{\beta} + MR^2\dot{\alpha}\left[\frac{3}{20}\dot{\alpha}c\beta + \frac{2}{5}\dot{\gamma}\right]s\beta + MgRc\beta = -\lambda_1 Rs\alpha s\beta + \lambda_2 Rc\alpha s\beta \tag{43}$$

$$\frac{2}{5}MR^2(\ddot{\gamma} - \dot{\alpha}\dot{\beta}\sin\beta + \ddot{\alpha}\cos\beta) = -\lambda_1 Rc\alpha - \lambda_2 Rs\alpha \tag{44}$$

The nonlinear differential equations (40) through (44), along with the constraint equations (18) and (19) completely describe the motion for the Gyrover wheel. Below, we analyze as well as numerically simulate these equations of motion.

3.2 Precession rate

Here we derive the effective steady precession rate for Gyrover as a function of the radius of curvature ρ, the radius of the wheel R, the lean angle β, and the gravitational acceleration g. For different gravitational environments, such as on earth, the moon, or Mars, this information can be important for the automatic control of Gyrover.

To achieve steady precession (i.e. $\ddot{\alpha} = 0$), the center of the wheel must follow a circular path with radius of curvature ρ and constant lean angle β, such that $\dot{\beta} = 0$. Assume that the motion is centered about the z-axis of the inertial frame, such that,

$$X = -\rho s\alpha, Y = \rho c\alpha. \tag{45}$$

Letting $\ddot{\alpha} = 0$ and $\dot{\beta} = 0$, the conditions for steady precision, the constraint equations (18) and (19) reduce to,

$$\dot{X} = R(\dot{\gamma} + \dot{\alpha}c\beta)c\alpha, \dot{Y} = R(\dot{\gamma} + \dot{\alpha}c\beta)s\alpha \tag{46}$$

Differentiating equations (45) with respect to time, we get,

$$\dot{X} = -\rho\dot{\alpha}c\alpha, \dot{Y} = -\rho\dot{\alpha}s\alpha. \tag{47}$$

Setting equations (46) and (47) equal to one another,

$$\left(-\frac{\rho}{R}\right)\dot{\alpha} = \dot{\gamma} + \dot{\alpha}c\beta \tag{48}$$

$$-\left(\frac{\rho}{R} + \cos\beta\right)\dot{\alpha} = \dot{\gamma} \tag{49}$$

Thus, equations (45) will be satisfied for the Lagrangian equations of motion under the condition given by equation (49). Next, differentiating equations (46) with respect to

time and combining with equations (40) and (41), we get that,

$$\lambda_1 = M\rho(-\ddot{\alpha}c\alpha + \dot{\alpha}^2 s\alpha) \tag{50}$$

$$\lambda_2 = M\rho(-\ddot{\alpha}s\alpha - \dot{\alpha}^2 c\alpha). \tag{51}$$

Finally, combining equations (42), (50) and (51) and solving for $\dot{\alpha}$, we derive the desired relationship to be,

$$\dot{\alpha}^2 = \frac{20g\cot\beta}{5R\cos\beta + 28\rho} \tag{52}$$

The corresponding velocity of the wheel's center is given by $v^2 = (\rho\dot{\alpha})^2$,

$$v^2 = \frac{20g\cot\beta\rho^2}{5R\cos\beta + 28\rho} \tag{53}$$

Figures 5 and 6, plot the velocity v as a function of the radius of curvature ρ and the lean angle β, respectively, for gravitational accelerations corresponding to those of earth, Mars, and the moon. Note that for Mars and moon, whose gravitational accelerations are approximately one third and one sixth that of earth, respectively, the Gyrover wheel can be driven at significantly higher velocities through tighter turns. Also, the wheel will be relatively more stable in a lunar or Martian environment, as demonstrated by the smaller lean angles as shown in Figure 6.

4. Simulation experiments

We have solved the equations of motion numerically and simulated them for $M = 2\text{kg}$ and $R = 17\text{cm}$, and initial conditions $x_0 = 0$, $y_0 = 0$, $\alpha_0 = 0$, $\beta_0 = 80\text{deg}$, $\gamma_0 = 0$, $\dot{x}_0 = 0$, $\dot{y}_0 = 0$, $\dot{\alpha}_0 = 0$, $\dot{\beta}_0 = 0$, $\dot{\gamma}_0 = 6$ rad/s. We compare the resulting motion for gravitational accelerations g corresponding to earth, Mars and the moon.

Figures 7, 8, and 9 plot the state trajectories for a period of 20 seconds on earth, Mars, and the moon, respectively, in order of decreasing gravitational acceleration g. First, note the trajectory of the wheel on earth (Figure 7). The wheel wobbles significantly back and forth, as shown by the large variations in the lean angle β, and the irregularly shaped x-y trajectory. Now compare the trajectory on earth to that on Mars (Figure 8) and the moon (Figure 9). On Mars, the wheel precesses in a nearly perfect circular path of larger radius than on earth, and will take significantly longer than 20 seconds to eventually fall down. The x-y trajectory on the moon traces an even larger circle (twice the diameter of Mars' circle) and the wheel will take even longer to fall down in that gravitational field. Thus, we expect that a single-wheel robot such as Gyrover will have significantly greater dynamic stability as a planetary rover on either Mars or the moon rather than earth.

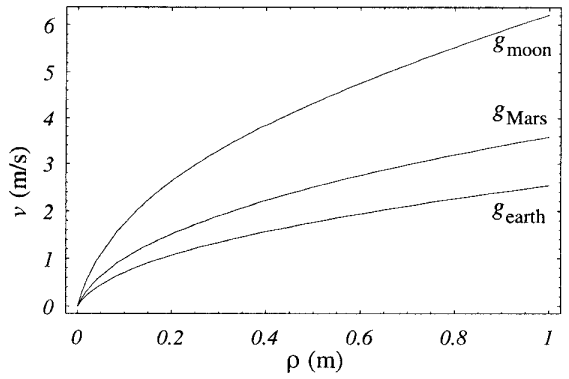

Fig. 5: Variations in the velocity as a function of the radius of curvature and different gravitational forces.

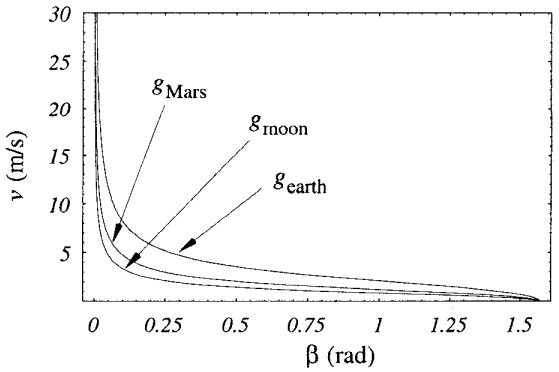

Fig. 6: Variations in the velocity for different lean angles and different gravitational forces (earth, Mars, and moon).

5. Conclusion

In this paper, we have developed a dynamic model of a gyroscopic wheel, utilizing the constrained generalized Lagrangian principle for nonholonomic systems. We have implemented the equations of motion in a real-time graphic simulator, and have simulated the dynamic behavior of the wheel for different initial conditions and different gravitational environments, such as those seen on the moon, and Mars. From these simulations, we have seen that the unactuated gyroscopic wheel has greater stability in lower gravitational fields, but ultimately needs additional actuation to maintain indefinite stability. The work in this paper is an important first step in the theoretical analysis and control of the single wheel Gyrover robot, developed at Carnegie Mellon University.

Acknowledgments

We thank Michael C. Nechyba for his help in simulating the equations of motion. We also thank Joseph Chan and W. Fung for their help in generating Figures 3 and 4.

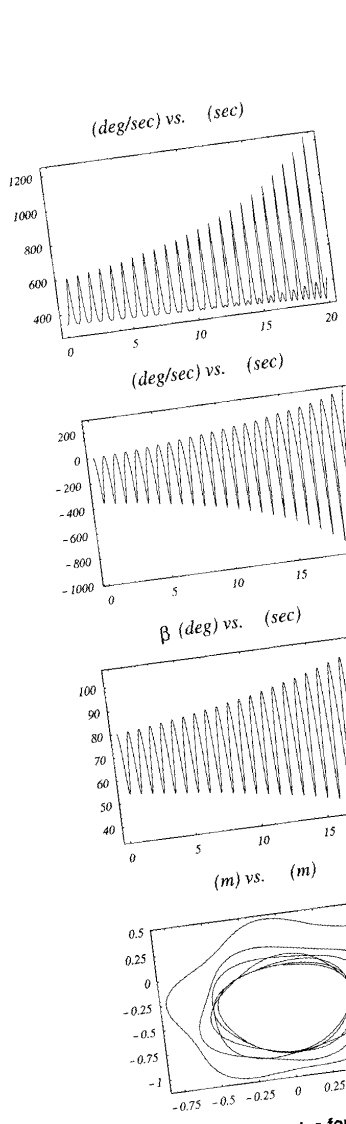

Fig. 7: State trajectories for earth's gravity.

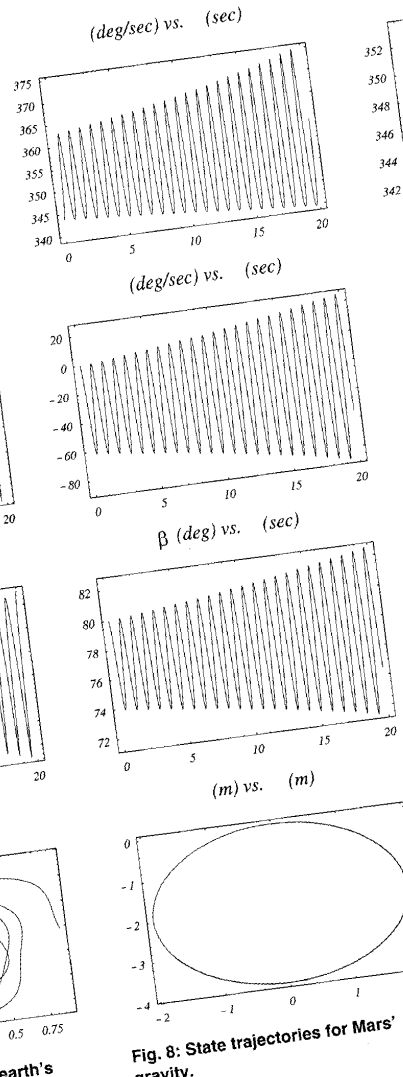

Fig. 8: State trajectories for Mars' gravity.

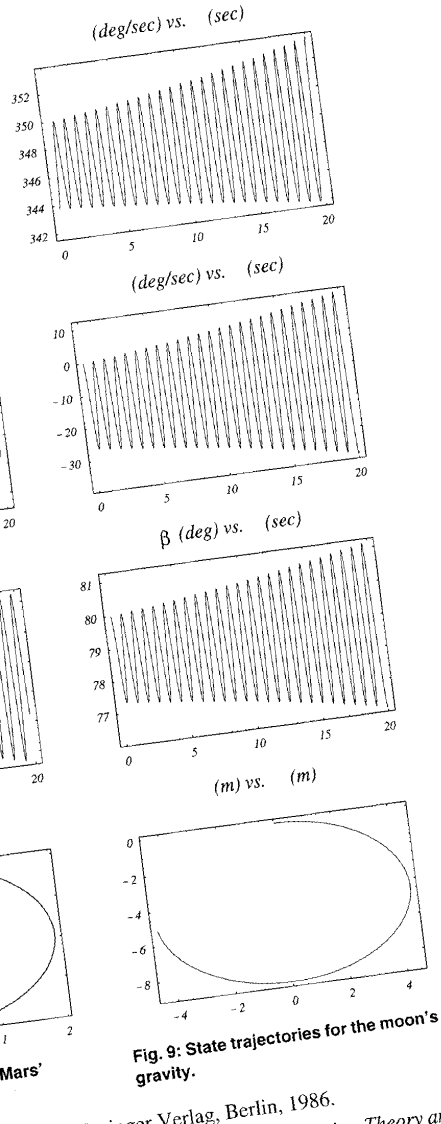

Fig. 9: State trajectories for the moon's gravity.

References

[1] H. B. Brown and Y. Xu, "A single wheel gyroscopically stabilized robot," *Proc. IEEE Int. Conf. on Robotics and Automation*, vol. 4, pp. 3658-63, 1996.

[2] Y. Xu, G. C. Nandy, M. C. Nechyba and H. B. Brown, "Analysis of Actuation and Dynamic Balancing For a Single Wheel Robot," submitted to *Int. Conf. on Robotics and Automation*, 1998.

[3] G. Bianchi and W. Schiehlen, *Dynamics of Multibody Systems*, Springer Verlag, Berlin, 1986.

[4] T.R. Kane and D. A. Levinson, *Dynamics, Theory and Applications*. McGraw-Hill, New York, 1985.

[5] R. L. Huston, *Multibody Dynamics*, Butterworth-Heinemann, Boston, 1990.

[6] J. H. Ginsberg, *Advanced Engineering Dynamics*, Cambridge University Press, Cambridge, 1995.

[7] H. Goldstein, *Classical Mechanics*, 2nd ed., Addison-Wesley, Reading, Massachusetts, 1980.